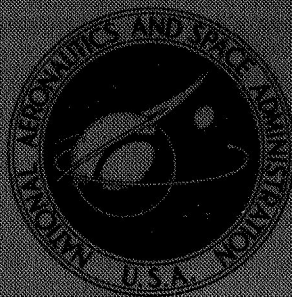


NASA TECHNICAL  
MEMORANDUM



NASA TM X-1514

NASA TM X-1514

GPO PRICE \$ \_\_\_\_\_

CSFTI PRICE(S) \$ \_\_\_\_\_

Hard copy (HC) 3.00

Microfiche (MF) .65

ff 653 July 65

FACILITY FORM 602

N 68-19347

(ACCESSION NUMBER)

(THRU)

20

(PAGES)

1

(CODE)

17

(CATEGORY)

(NASA CR OR TMX OR AD NUMBER)

EFFECT OF SURFACE ROUGHNESS ON THE  
0.66-MICRON NORMAL SPECTRAL EMITTANCE  
OF VAPOR-DEPOSITED RHENIUM FROM  
1500° TO 2100° K

*by Peter Cipollone*

*Lewis Research Center*

*Cleveland, Ohio*

NATIONAL AERONAUTICS AND SPACE ADMINISTRATION • WASHINGTON, D. C. • MARCH 1968

NASA TM X-1514

EFFECT OF SURFACE ROUGHNESS ON THE 0.66-MICRON NORMAL  
SPECTRAL EMITTANCE OF VAPOR-DEPOSITED  
RHENIUM FROM 1500<sup>0</sup> TO 2100<sup>0</sup> K

By Peter Cipollone

Lewis Research Center  
Cleveland, Ohio

NATIONAL AERONAUTICS AND SPACE ADMINISTRATION

---

For sale by the Clearinghouse for Federal Scientific and Technical Information  
Springfield, Virginia 22151 - CFSTI price \$3.00

EFFECT OF SURFACE ROUGHNESS ON THE 0.66-MICRON NORMAL  
SPECTRAL EMITTANCE OF VAPOR-DEPOSITED  
RHENIUM FROM 1500° TO 2100° K

by Peter Cipollone  
Lewis Research Center

SUMMARY

The normal spectral emittance of vapor-deposited rhenium at a 0.66-micron effective wavelength is presented, and the results are compared to previously published data on bar and sheet rhenium. A dependence of the normal spectral emittance on surface roughness is demonstrated quantitatively.

INTRODUCTION

Nondestructive determination of surface temperature distributions may be accomplished with knowledge of the surface spectral emittance. The determination of surface temperature distributions of thermionic emitters prior to their use in a cesiated converter is usually accomplished in this manner.

The normal spectral emittance of rhenium is reported in references 1 and 2, but in both cases specific information regarding the surface characteristics of the test samples was not given. The data of reference 1 were obtained from a thin rhenium sheet rolled into a tube, and the data of reference 2 were obtained from a hollow cylinder machined from solid rhenium bar stock. Except for the description "ground and polished" in regard to the specimen of reference 2, neither report contains any information regarding the condition of the surface for which the emittance was measured.

In reference 3 an attempt was made to establish a relation between emittance and surface roughness, but this attempt proved unsuccessful, possibly because of the low precision of the optical pyrometer used in the investigation.

In reference 4 the effects of surface roughness on the normal spectral emittance of tungsten were investigated, and although no definite trend was established, an increase of 20 to 50 percent in the emittance of roughened specimens was observed. It was concluded that, "The impracticability of preparing a roughened surface on one side of the very thin specimen while the other side remained ideal did not permit the use of the single specimen configuration for relative emittance ratio determination. If this diffi-

culty could be overcome, use of the apparatus with single specimen configuration to determine the relative emittance ratio could yield results with uncertainties less than 4 percent. The fact that the temperatures of the surfaces were not directly determined contributed to the greater uncertainties in the results for the double specimen configuration."

The measurements reported herein were made on a single hollow tantalum cylinder on the outside of which a thin layer of rhenium was vapor deposited. Prior to the emittance investigation, the cylinder had been heated with a helical electron-bombardment filament, and variations in crystal size and surface roughness were observed. The surface roughness was then measured at three positions, and flat-bottomed cylindrical hohlraums were spark-discharge machined at each location. At each position, temperature was measured by means of a disappearing-filament optical-brightness pyrometer. Mean normal spectral emittance values were compared for the three locations over the temperature range of 1500° to 2100° K at an effective-wavelength of 0.66 micron.

## SYMBOLS

$A_m$	mean area of cylinder through which heat flows radially
$c_1$	first radiation constant, $2\pi hc^2$ , $3.7405 \times 10^{-20} \text{ W-cm}^2$
$c_2$	second radiation constant, $1.43879 \text{ cm}^\circ\text{K}$
$D$	cavity diameter, cm
$D_1$	inside diameter of tantalum cylinder, cm
$D_2$	outside diameter of tantalum cylinder, cm
$k_m$	mean thermal conductivity, $k_m = 1/(T_2 - T_1) \int_{T_1}^{T_2} k \, dT$
$L$	cavity depth, cm
$l$	tantalum cylinder length, cm
$R_\lambda$	spectral radiance, $\text{W}/(\text{cm}^3)(\text{sr})$
$S_b$	brightness temperature, $^\circ\text{K}$
$T$	temperature, $^\circ\text{K}$
$Q$	total heat flux, W
$t$	tantalum cylinder wall thickness, cm
$\beta$	fractional uncertainty in value of $T$
2	

$\epsilon_{\lambda c}$	cavity spectral emittance
$\epsilon_{\lambda n}$	normal spectral emittance
$\epsilon_{\lambda w}$	cavity-wall normal spectral emittance
$\lambda$	wavelength, cm
$\nu$	fractional uncertainty in value of $\epsilon_{\lambda n}$

## APPARATUS AND PROCEDURE

### Test Fixture

A hollow cylinder machined from a tantalum rod and coated with a thickness of 0.028 centimeter of rhenium by the hydrogen reduction of rhenium hexafluoride was used in the investigation. The rhenium vapor deposition was performed by San Fernando Laboratories, Pacoima, California. The cylinder is shown mounted in the test fixture in figure 1. The heated length was 3.94 centimeters, and the cylinder was 1.326 centimeters in diameter with a total wall thickness of 0.229 centimeter. The cylinder was heated by bombardment with electrons from a helical tungsten filament.

The device was tested in a molecular-adsorption and ion-pumped vibration-free vacuum system at pressures ranging from  $1 \times 10^{-6}$  to  $5 \times 10^{-6}$  torr ( $1.33 \times 10^{-4}$  to  $6.67 \times 10^{-4}$  N/m<sup>2</sup> abs). During the test, temperature variations of 150° to 200° K existed at all times axially along the cylinder with the midregion being the hottest and the top of the cylinder being the coolest. After approximately 50 hours of operation, a difference in crystal size and regularity became apparent. After an additional 170 hours of operation, photomicrographs were taken of the cylinder surface (fig. 2). Surface roughness (measured by a traverse parallel to the direction of surface grinding) and grain size were also measured at three locations; these measurements are presented in table I. The rms surface roughness ranged from a maximum of 55.0 microinches (1.397 microns) at the center of the cylinder to a minimum of 32.5 microinches (0.825 micron) at the top of the

TABLE I. - MEASUREMENTS OF CYLINDER AND CAVITY

Cavity	Cavity axial position, cm	Cavity diameter, cm	Cavity depth to diameter ratio	Surface roughness		Grain size (ASTM)
				$\mu$ in.	microns	
Top	0.521	0.046	2.5	32.5	0.825	2 to 8 (Duplex)
Middle	2.202	.036	3.45	55.0	1.397	3 (Uniform)
Bottom	3.818	.030	4.1	45.0	1.143	3 to 7 (Duplex)

cylinder. The grain size ranged from ASTM 2 to 8 and was duplex at the top and bottom region and uniform in the center.

The cylinder was then prepared for surface-temperature determination. Three flat-bottomed hohlraums were spark-discharge machined into the surface of the cylinder. The cavities were 0.521, 2.202, and 3.818 centimeters from the top of the 3.94-centimeter-long heated section of the cylinder (fig. 3). (At these axial locations the photomicrographs of fig. 2 were taken.) After machining, the cavity depths and diameters were measured with an optical comparator. The cavity dimensions are also presented in table I.

Although it was intended to have identical geometries for all three cavities (0.254-mm diam, 1.016-mm depth), difficulty in controlling the diameter of small holes when spark-discharge machining through recrystallized rhenium made this impossible. Larger cavity-depth to diameter ratios were not permitted because of both the limited thickness of the cylinder wall and the limited optical resolution of the pyrometer.

## Temperature Determination

By means of a disappearing-filament optical pyrometer, temperature was measured at the bottom of each of the three hohlraums listed in table I and on the vapor-deposited rhenium surface immediately adjacent to each cavity. Data were accumulated at temperatures between 1500° and 2100° K.

Because optical-brightness pyrometers are not truly monochromatic, the observed brightness temperature corresponds to an effective wavelength that is temperature dependent. For the instrument used, the effective wavelengths varied from 0.6602 to 0.6582 micron for temperatures from 1500° to 2100° K, respectively.

Cavity emittance was estimated from the cavity geometry (table I), the cavity-wall emittance as determined from equation (1) of appendix A, and the cavity-emittance equations of reference 5. With these cavity emittance values and the measured cavity-brightness temperatures as input to equation (1) of appendix B, true cavity-end disk temperatures were obtained. Hohlraum temperature was then adjusted for the radial temperature difference in the cylinder wall (appendix A) from the bottom of the cavity to the rhenium surface. These true surface temperatures and the corresponding rhenium surface-brightness temperatures were then used with equation (1) of appendix B in order to determine the normal spectral emittance of the rhenium surface.



## Error Analysis

An extensive review of the error factors involved in optical-pyrometer temperature measurements is presented in reference 6. This study is concerned with comparing measurements made under identical conditions (i. e., one instrument, one operator, one heat source, etc.) except for the conditions of the rhenium surface. Therefore, the precision (or reproducibility of measurement) rather than absolute accuracy (or degree of agreement with correct values) is of primary importance. The factors that may reduce the precision of the optical temperature measurements are instrument error, observer error, and errors associated with the determination of the emittance of shallow hohlraums. Each of these factors is discussed in the following paragraphs. Since the same optical viewpath was used for all data, glassware corrections were the same and thus did not affect the precision of readings for the three locations.

The milliammeter normally used with the pyrometer is directly calibrated in increments of either  $5^{\circ}$  or  $10^{\circ}$  C, depending on the instrument scale used. To minimize instrument readout error, the milliammeter was replaced with a four-place digital voltmeter. The pyrometer output was shunted across a calibrated 1.0-ohm ( $\pm 0.1$  percent) resistor. The improved instrument readout precision achieved is apparent in that the maximum slope of the calibration curve of the instrument is 0.098 millivolt per  $^{\circ}$ K. Since the digital voltmeter has the capability of measuring to the nearest 0.1 millivolt, the maximum instrument readout error is  $\pm 1^{\circ}$  K.

The error associated with the observer in optical-brightness pyrometry is not as easily defined as the instrument readout error. Studies of single-observer random errors and systematic errors associated with more than one observer are reported in references 6 and 7. Under the nearly ideal conditions (i. e., completely blacked-out room, etc.) that existed during these tests, the random error associated with a single observer would be less than  $\pm 2^{\circ}$  K for temperature measurements to  $2500^{\circ}$  K, as shown in reference 7.

From these error considerations, it may be concluded that cavity-emittance corrections are appropriate for a comparison of the cavities if the difference between the cavity brightness and true temperatures is much greater than  $3^{\circ}$  K.

At  $1500^{\circ}$  and  $2100^{\circ}$  K the ratios of the uncertainty in true temperature to the uncertainty in emittance (from appendix B) are 0.069 and 0.095, respectively, that is,

$$\left. \begin{array}{l} \frac{\beta}{\nu} \Big|_{T=1500^{\circ}\text{K}} = 0.069 \\ \frac{\beta}{\nu} \Big|_{T=2100^{\circ}\text{K}} = 0.095 \end{array} \right\} \quad (1)$$

If temperature error  $\Delta T$  is assumed to be  $3^{\circ}\text{K}$  in each case,

$$\left. \begin{aligned} \nu_{T=1500^{\circ}\text{K}} &= 0.029 \\ \nu_{T=2100^{\circ}\text{K}} &= 0.015 \end{aligned} \right\} \quad (2)$$

Since ideal cavity emittance is 1, the emittance corrections are necessary at  $1500^{\circ}$  and  $2100^{\circ}\text{K}$  if the calculated cavity emittances are less than the values shown in table II.

TABLE II. - MINIMUM APPROPRIATE  
CAVITY SPECTRAL EMITTANCE

Cavity spectral emittance, $\epsilon_{\lambda c}$	Temperature, $^{\circ}\text{K}$
0.971	1500
.985	2100

Analytical procedures for determining the emittance of shallow blackbody cavities are described in references 5 and 8 to 14. An experimental evaluation of the various cavity-emittance correction procedures was not conducted during these tests, and the selection of the particular procedure used is based on the work reported in reference 7. The shallow-cavity analytical correction procedure recommended in reference 7 and selected as being the most suitable for use with these data is that of reference 5.

The cavity emittances for the cavity-end disk of the top, middle, and bottom cavities (table I) were computed by the cavity-emittance correction procedure of reference 5 and

TABLE III. - CAVITY EMITTANCE  
VALUES FOR TRUE  
TEMPERATURES

Cavity	Temperature, $^{\circ}\text{K}$	
	1500	2100
	Cavity emittance	
Top	0.954	0.955
Middle	.977	.978
Bottom	.985	.985



the cavity-wall emittance values determined by the method described in appendix A. These values are presented in table III for true temperatures of 1500<sup>0</sup> and 2100<sup>0</sup> K.

Comparison of the results of table II with those of table III indicates that cavity-emittance values are not sufficiently high for the top cavity at 1500<sup>0</sup> K and the top and middle cavities at 2100<sup>0</sup> K to exclude the need for emittance corrections. In these cases, cavity-emittance corrections were applied to the data by the procedure presented in reference 7.

The absolute accuracy of the data reported herein may be no better than that of previously published works (refs. 3 and 4) in which attempts were made to relate surface conditions to emittance. However, the experimental conditions in this study were such that the precision of temperature measurement, estimated to be  $\pm 3^0$  K, is better than that previously achieved.

## RESULTS AND DISCUSSION

The normal spectral emittance values for the vapor-deposited rhenium surface at three axial locations are presented in figure 4. The bands shown represent the degree of precision anticipated in the section Error Analysis (i. e.,  $\partial T = 3^0$  K where  $\nu/\beta$  varies from -14.5 at 1500<sup>0</sup> K to -10.5 at 2100<sup>0</sup> K).

The means of the bands of figure 4 are plotted in figure 5 where the data of references 1 and 2 are also shown. A substantial difference exists among the data from the three sources. Different types of rhenium were used for the three investigations, namely, thin sheet rhenium in reference 1, solid bar stock in reference 2, and vapor-deposited rhenium in this investigation. For vapor-deposited rhenium with 55.0-microinch (1.397-micron) surface roughness, the mean emittance decreases from 0.509 at 1500<sup>0</sup> K to 0.444 at 2100<sup>0</sup> K, whereas at 32.5-microinch (0.825-micron) surface roughness, the mean emittance decreases from 0.458 at 1500<sup>0</sup> K to 0.404 at 2100<sup>0</sup> K.

In figure 6, mean emittance values for vapor-deposited rhenium are plotted as a function of surface roughness with true surface temperature as a parameter. This figure indicates a dependence of the mean normal spectral emittance on the surface roughness. For example, at 1800<sup>0</sup> K the emittance increases from 0.430 at a surface roughness of 32.5 microinches (0.825 micron) to 0.477 at a surface roughness of 55.0 microinches (1.397 microns). Also shown in figure 6 are error bars based on the precision bands of figure 4.

Thus, there appears to be a definite dependence of the normal spectral emittance on the surface roughness, and this difference is detectable with standard optical-pyrometry equipment.

## CONCLUDING REMARKS

The dependence of the normal spectral emittance of vapor-deposited rhenium on surface roughness was experimentally investigated for specimen temperatures of  $1500^{\circ}$  to  $2100^{\circ}$  K. A cylindrical specimen, having an axial variation in surface roughness from 0.825 to 1.397 microns, was used. The surface emittance was determined from measured values of surface brightness and hohlraum temperatures. The results indicate a dependence of emittance on surface roughness.

Lewis Research Center,  
National Aeronautics and Space Administration,  
Cleveland, Ohio, November 1, 1967,  
120-27-05-01-22.

## APPENDIX A

### CAVITY-WALL EMITTANCE AND AXIAL CAVITY TEMPERATURE

#### GRADIENT CALCULATIONS

##### Cavity-Wall Emittance

It is shown in reference 5 that in order to determine the cavity emittance, both the cavity geometry (L/D) and the cavity-wall emittance must be known. Because the cavity walls in the test device consisted of both rhenium and tantalum, an average cavity-wall emittance was determined by applying averaging factors based on the percentage of cavity-wall area of each of the two metals. These percentages are presented in the following table for the three cavities.

Cavity	Rhenium	Tantalum
	Cavity-wall area, percent	
Top	22.2	77.8
Middle	21.4	78.6
Bottom	21.2	78.8

Next, the normal spectral emittance values for both rhenium and tantalum in the temperature range of 1500<sup>0</sup> to 2100<sup>0</sup> K at an effective wavelength of 0.66 micron were required. There are several experimental determinations of tantalum normal spectral emittance as noted in references 15 to 19. The data of reference 19 were used as a source for tantalum emittance values. Experimental data on rhenium normal spectral emittance are more limited than those for tantalum. Values reported in references 1 and 2 are presented in figure 5. Since the spark-discharge-machining method of cavity manufacture produced highly diffuse cavity walls, the rhenium data of reference 2 were believed to be more representative of the conditions that existed in this test.

The cavity-wall emittance was determined from the following equation:

$$\epsilon_{\lambda w} = \frac{(\text{Percentage of Re area})\epsilon_{\lambda n, \text{Re}} + (\text{Percentage of Ta area})\epsilon_{\lambda n, \text{Ta}}}{100} \quad (\text{A1})$$

The  $\epsilon_{\lambda w}$  values were identical to three significant figures for the cavities between 1500<sup>0</sup> and 2100<sup>0</sup> K. The values ranged from 0.428 at 1500<sup>0</sup> K to 0.437 at 2100<sup>0</sup> K. With

these emittance values and the measured cavity geometries, the cavity emittance was then determined from the cavity-emittance equations of reference 5.

### Cavity Axial Temperature Gradients

Since the hollow tantalum cylinder was heated internally by electron bombardment, a temperature gradient existed across the cylinder wall and, thus, between the cavity-end disks and the rhenium surface. From the equation

$$Q = k_m A_m \frac{2 \Delta T}{(D_2 - D_1)} \quad (A2)$$

the temperature drop  $\Delta T$  across the cylinder wall may be calculated as a function of the total heat input  $Q$ . Since,  $D_1 = 0.869$  centimeter,  $D_2 = 1.326$  centimeters, and  $l = 3.94$  centimeters,

$$A_m = \frac{\pi D_2 l - \pi D_1 l}{\ln \frac{D_2}{D_1}} = 13.400 \text{ cm}^2 \quad (A3)$$

$$\Delta T = \frac{(D_2 - D_1)}{2k_m A_m} Q = 0.0172 \frac{Q}{k_m} \quad (A4)$$

From reference 20, the mean thermal conductivity of tantalum  $k_m$  over the temperature range considered is 0.801 watt per centimeter  $^{\circ}\text{K}$ . Since the thickness of rhenium was only 12 percent of the total cylinder wall thickness, the entire 0.229-centimeter wall was considered to be tantalum for this calculation. Therefore, equation (4) reduces to

$$\Delta T = 0.0215 Q \quad (A5)$$

For each set of data, the input power  $Q$  was measured with an estimated accuracy of  $\pm 10$  percent. The temperature difference across the cylinder wall was determined for all the cavity-temperature measurements made. Because the wall was thin, it was assumed that a linear temperature gradient existed across it, that is,

$$\frac{\Delta T}{t} = 0.094 Q \quad (A6)$$

For example, the power input for a temperature of approximately 1500° K at the middle cavity position was 450 watts. Thus,

$$\frac{\Delta T}{t} = 0.094(450) = 42.3 \quad (A7)$$

Since the middle cavity is 0.122 centimeter in depth (see table I), the  $\Delta T$  from the cavity bottom to the surface would be 5° K. This correction was applied to the observed temperature. In a similar fashion, corrections were applied to the top and bottom cavity data.

## APPENDIX B

### RELATION OF ERROR IN EMITTANCE TO ERROR IN TRUE TEMPERATURE

The equation

$$\ln \epsilon_{\lambda n} = \frac{c_2}{\lambda} \left( \frac{1}{T} - \frac{1}{S_b} \right) \quad (B1)$$

which relates the true and brightness temperatures to the spectral emittance and wavelength is derived from Wien's equation

$$R_{\lambda} = \frac{c_1 \lambda^{-5}}{e^{\frac{c_2}{\lambda T}}} \quad (B2)$$

in reference 7.

If equation (B1) is differentiated with respect to  $T$ ,

$$\frac{1}{\epsilon_{\lambda n}} \frac{\partial \epsilon_{\lambda n}}{\partial T} = - \frac{c_2}{\lambda T^2} \quad (B3)$$

or

$$\frac{\nu}{\beta} = - \frac{c_2}{\lambda T} \quad (B4)$$

Thus, the ratio of emittance error to temperature error is inversely proportional to  $\lambda T$ .

Evaluation of this ratio at temperatures of  $1500^{\circ}$  and  $2100^{\circ}$  K indicates that at  $1500^{\circ}$  K the uncertainty in emittance is 14.5 times greater than the uncertainty in temperature and decreases to approximately 10 at  $2100^{\circ}$  K, as shown in figure 7.

## REFERENCES

1. Marple, D. T. F.: Spectral Emissivity of Rhenium. *J. Optical Soc. Am.*, vol. 46, no. 7, July 1956, pp. 490-494.
2. Sims, C. T.; Craighead, C. M.; Jaffee, R. I.; Gideon, D. N.; Wyler, E. N.; Todd, F. C.; Rosenbaum, D. M.; Sherwood, E. M.; and Campbell, I. E.: Investigations of Rhenium. Battelle Memorial Inst. (WADC TR-54-371), June 1954.
3. Stark, B. V.; and Shashkov, Yu. M.: The Effect of Surface Roughness and of Film on Solid and Liquid Metals on the Accuracy of Optical Measurements of Temperature. *Izvest. Akad. Nauk SSSR Otdel. Tekh. Nauk*, no. 3, 1952, pp. 395-404.
4. DeWitt, David P.: The Effect of Surface Roughness on the Normal Spectral Emissivity of Tungsten. Ph. D. Thesis, Purdue University, 1963.
5. Sparrow, E. M.; Albers, L. U.; and Eckert, E. R. G.: Thermal Radiation Characteristics of Cylindrical Enclosures. *J. Heat Transfer*, vol. 84, no. 1, Feb. 1962, pp. 73-81.
6. Kostkowski, H. J.; and Lee, R. D.: Theory and Methods of Optical Pyrometry. Monograph No. 41, National Bureau of Standards, Mar. 1, 1962.
7. Branstetter, J. Robert: Some Practical Aspects of Surface Temperature Measurements by Optical and Ratio Pyrometers. NASA TN D-3604, 1966.
8. Buckley, H.: On Radiation From the Inside of a Circular Cylinder. *Phil. Mag.*, vol. 4, Oct. 1927, pp. 753-762.
9. Gouffe, A.: Aperture Corrections for Artificial Blackbodies, Taking Account of Multiple Internal Reflections. *Rev. Opt. (Théor. Instrum.)*, vol. 24, Jan.-Mar. 1946, pp. 1-10.
10. DeVos, J. C.: Evaluation of the Quality of a Blackbody. *Physica*, vol. 20, 1954, pp. 669-689.
11. Edwards, David F.: The Emissivity of a Conical Blackbody. Rep. No. 2144-105-T, University of Michigan, Nov. 1956.
12. Polgar, Leslie G.; and Howell, John R.: Directional Thermal-Radiative Properties of Conical Cavities. NASA TN D-2904, 1965.
13. Buckley, H.: On Radiation from the Inside of a Circular Cylinder. *Phil. Mag.*, vol. 6, Sept. 1928, pp. 447-457.



14. Buckley, H.: On Radiation from the Inside of a Circular Cylinder. Part III. Phil. Mag., vol. 17, Mar. 1934, pp. 576-581.
15. Parker, W. J.; and Abbott, G. L.: Theoretical and Experimental Studies of the Total Emittance of Metals. Symposium on Thermal Radiation of Solids. S. Katzoff, ed., NASA SP-55, 1965, pp. 11-28.
16. Riethof, T.; Acchione, B. D.; and Branyan, E. R.: High-Temperature Spectral Emissivity Studies on Some Refractory Metals and Carbides. Temperature - Its Measurement and Control in Science and Industry. Vol. 3, Part 2. Reinhold Publishing Corp., 1962, pp. 515-522.
17. Allen, Robert D.; Glasier, Louis F., Jr.; and Jordan, Paul L.: Spectral Emissivity, Total Emissivity, and Thermal Conductivity of Molybdenum, Tantalum, and Tungsten above 2300<sup>0</sup> K. J. Appl. Phys., vol. 31, no. 8, Aug. 1960, pp. 1382-1387.
18. Riethof, Thomas R.: High Temperature Spectral Emissivity Studies. Rep. No. R61SD004, General Electric Co., Jan. 1961.
19. Askwyth, W. H.; Hayes, R. J.; House, R. D.; and Mikk, G.: Determination of the Emissivity of Materials. Rep. No. PWA-2206, vol. III (NASA CR-56498), Pratt and Whitney Aircraft, 1962.
20. Goldsmith, Alexander; Waterman, Thomas E.; and Hirschhorn, Harry J.: Thermo-physical Properties of Solid Materials. Volume I - Elements (Melting Temperature Above 1000<sup>0</sup> F). Armour Research Foundation (WADD TR-58-476, vol. 1), Aug. 1960.

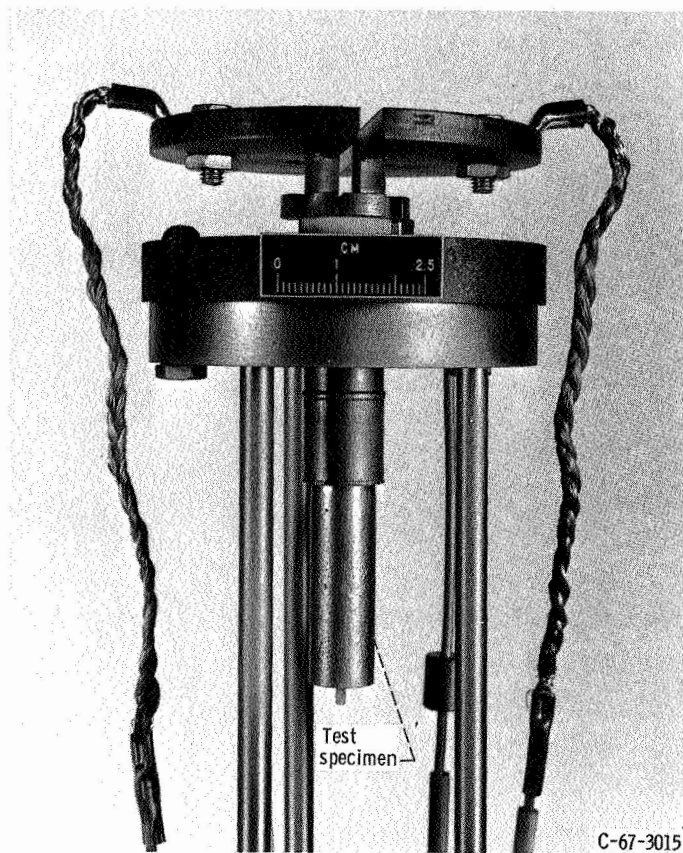
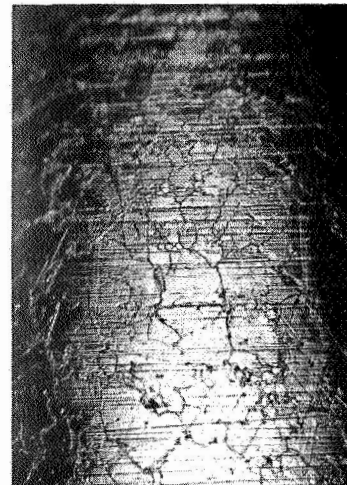
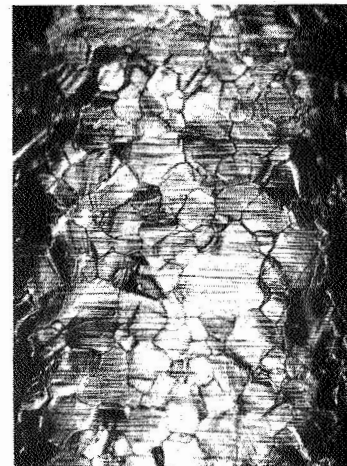


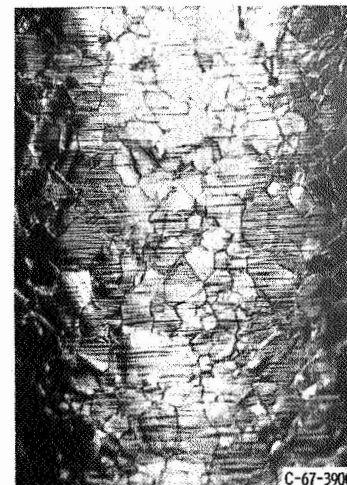
Figure 1. - Vapor-deposited rhenium cylinder mounted in test fixture.



(a) Top.



(b) Middle.



(c) Bottom.

Figure 2. - Rhenium surface at three cavity positions after 220 hours of operation. X50.

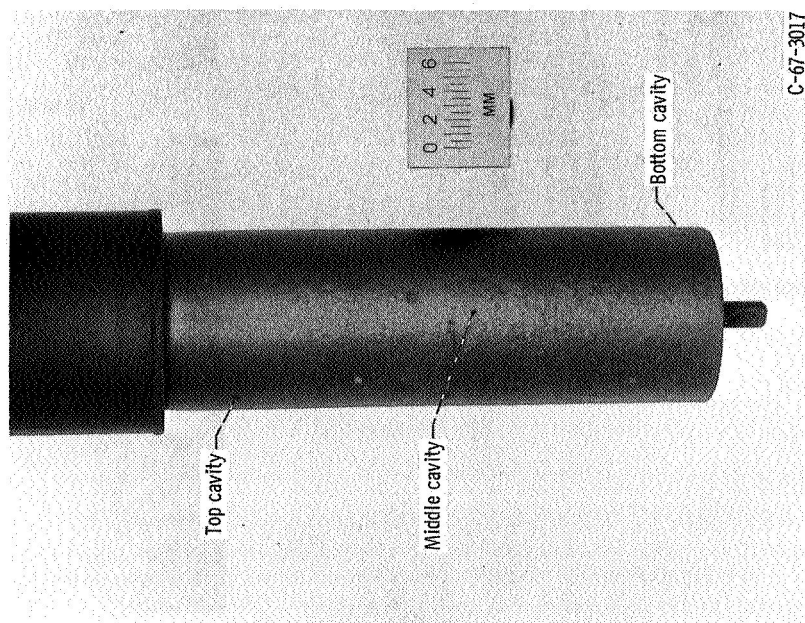


Figure 3. - Location of cavities machined in vapor-deposited rhenium surface.

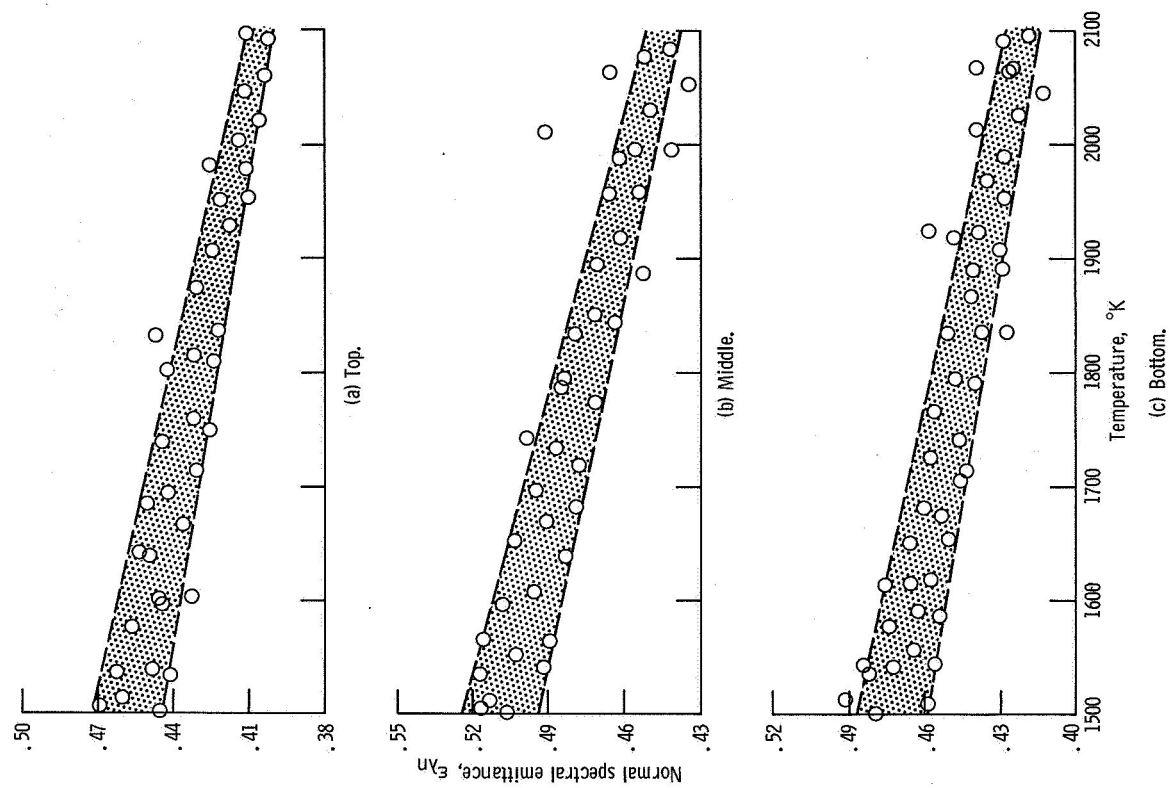


Figure 4. - Normal spectral emissivity of vapor-deposited rhenium as function of surface temperature at three different positions on test specimen.

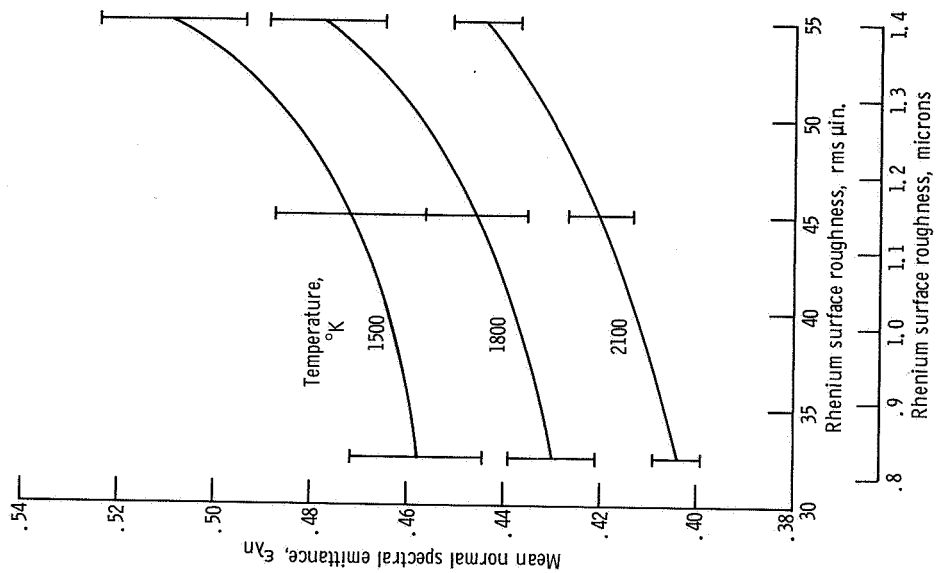


Figure 6. - Vapor-deposited rhenium mean normal spectral emissance as function of surface roughness at 1500°, 1800°, and 2100° K.

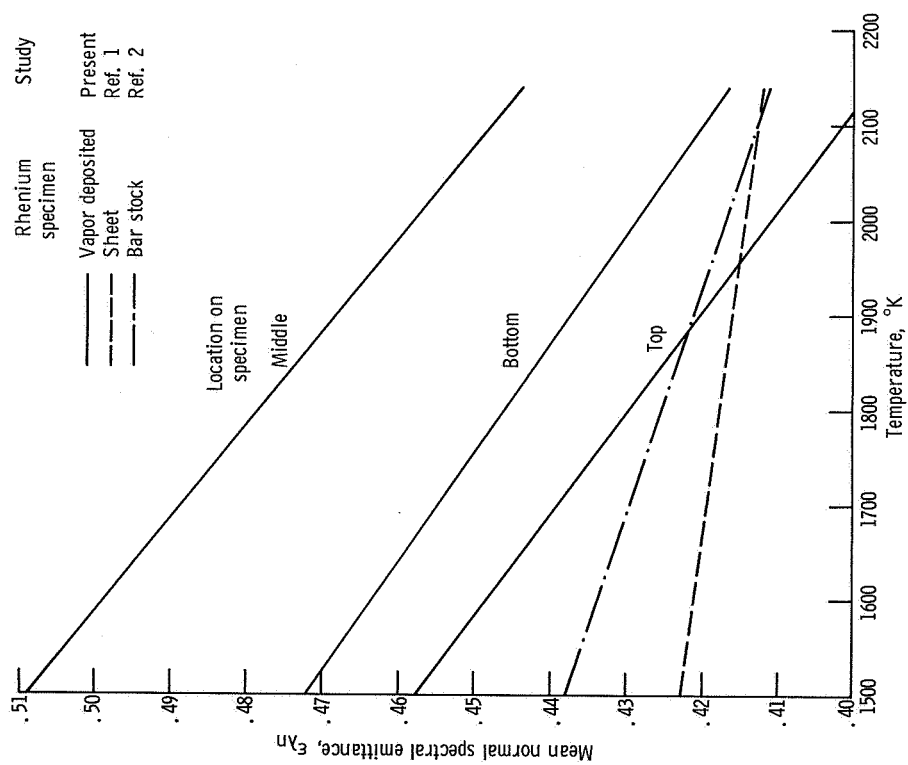


Figure 5. - Rhenium mean normal spectral emissance values for three positions compared with previously published data.

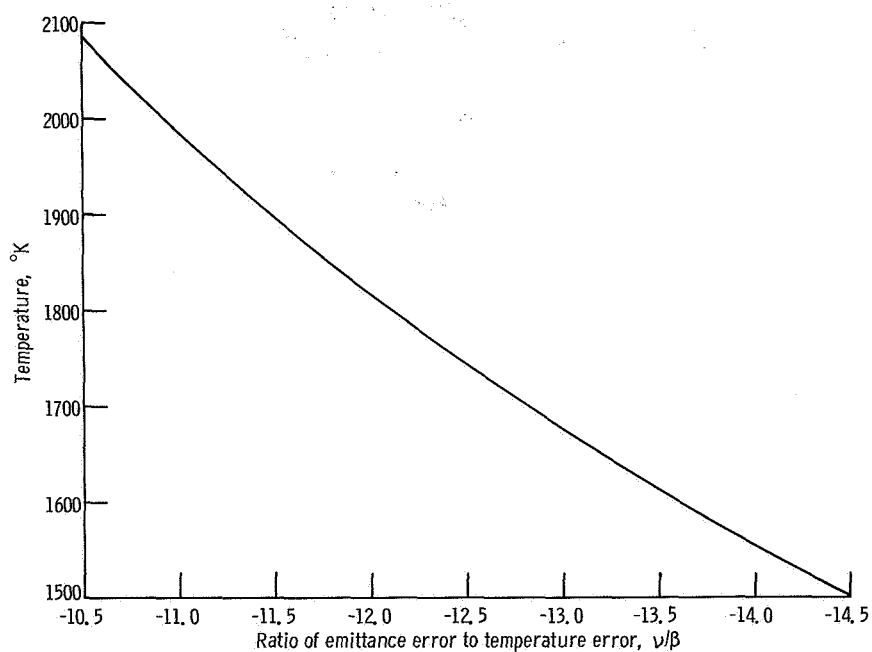


Figure 7. - Relation of emittance and temperature errors associated with use of Wien equation (appendix B).